A Simple and Direct Time Domain Derivation of the Dyadic Green's Function for a Uniformly Moving Non-Dispersive Dielectric-Magnetic Medium

Tatiana Danov and Timor Melamed

***Abstract*—The present contribution is concerned with deriving the relativistic electric and magnetic time-dependent dyadic Green's functions of an isotropic dielectric-magnetic medium (at the frame-at-rest) that is moving in a uniform relativistic velocity under the framework of the Minkowski constitutive relations. The results presented here correct previous reports in the literature [R. Compton, *J. Math. Phys.* 7, 2145 (1966)] and [C. Tai, *J. Math. Phys.* 8, 646 (1967)]. By applying a simple space-time and fields-sources transformation, scalarization of the vectorial problem is obtained. Thus the electromagnetic dyads are evaluated from the Green's function of the scalar (time-dependent) wave equation in free space. Emphasis is placed on a simple and direct time domain derivation.**

***Index Terms*—Čerenkov radiation, dyadic Green's function, moving medium, special relativity.**

I. Introduction and Statement of the Problem

In the late sixties, Compton [1] and Tai [2] have investigated the relativistic electric and magnetic time-dependent (TD) dyadic Green's functions (GFs) of an isotropic dielectric-magnetic medium that is moving in a fast uniform velocity. In [1] the dyadic GFs were derived by applying a four-fold (space-time) Fourier transform to the vector and scalar potentials. The dyadic GFs were obtained by applying operators to a scalar GF for which closed form analytic solution was given. In [2] a temporal Fourier transform was applied for obtaining the necessary scalar GF for the anisotropic medium (in the laboratory frame). Similar results were obtained in [3] by applying retarded potentials. Analytic solutions for the *time-harmonic* dyadic GFs in a moving medium have been a subject of continuous research for the past decades [4]–[7], and in recent years [8]–[11].

In the present contribution, we derive the dyadic GFs directly from the TD Maxwell's equations by using an elegant space-time and fields-sources normalization that transforms the vectorial problem into the standard procedure of obtaining the scalar isotropic (free-space) GF. Furthermore, the resulting GFs in the over phase-speed regime (Čerenkov radiation) are different from the ones that were obtained in [1]–[3] [see discussion following (30)].

Our aim is to obtain the TD dyadic GFs for medium that is moving in a uniform translation velocity $\mathbf{v} = v\hat{\mathbf{z}}$ where we assume with no loss of generality, that the velocity is in the direction of the z-axis. Unit vectors in the conventional cartesian coordinate system (x, y, z) are denoted by hat over bold fonts. The medium is assumed to be a linear isotropic non-dispersive dielectric-magnetic in the comoving frame, with ϵ_r and μ_r denoting its relative permittivity and permeability with respect to vacuum, respectively.

Manuscript received September 19, 2011; revised November 05, 2011; accepted November 08, 2011. Date of publication March 02, 2012; date of current version May 01, 2012.

The authors are with the Department of Electrical and Computer Engineering, Ben-Gurion University of the Negev, Beer Sheva 84105, Israel (e-mail: timormel@ee.bgu.ac.il).

Color versions of one or more of the figures in this communication are available online at http://ieeexplore.ieee.org.

Digital Object Identifier 10.1109/TAP.2012.2189745

Maxwell's TD curl equations that are corresponding to the Minkowski constitutive relations are given by [1]

$$\begin{aligned}\nabla \times \mathbf{E} &= -\mu_0\mu_r\partial_t \underline{\boldsymbol{\alpha}} \cdot \mathbf{H} + c^{-1} m \partial_t \hat{\mathbf{z}} \times \mathbf{E} \\ \nabla \times \mathbf{H} &= \epsilon_0\epsilon_r\partial_t \underline{\boldsymbol{\alpha}} \cdot \mathbf{E} + c^{-1} m \partial_t \hat{\mathbf{z}} \times \mathbf{H} + \mathbf{J}\end{aligned} \tag{1}$$

where $c = 1/\sqrt{\epsilon_0\mu_0}$ is the speed of light in vacuum,

$$\beta = v/c, \quad m = \beta\frac{n^2-1}{1-n^2\beta^2}, \quad n = \sqrt{\epsilon_r\mu_r} \tag{2}$$

and $\underline{\boldsymbol{\alpha}}$ is the diagonal matrix

$$\underline{\boldsymbol{\alpha}} = \mathrm{diag}\{\alpha, \alpha, 1\}, \quad \alpha = \frac{1-\beta^2}{1-n^2\beta^2}. \tag{3}$$

Here and henceforth underlined boldfaced letters denote dyadics/matrices.

II. Dyadic Green's Functions

A. General Formulation

The TD electric and magnetic Green's dyads, $\underline{\mathbf{G}}^e$ and $\underline{\mathbf{G}}^h$, perform a mapping from the current density sources $\mathbf{J}(\mathbf{r}, t)$ to the electric and magnetic vector fields by

$$\begin{aligned}\mathbf{E}(\mathbf{r}, t) &= -\mu_0\partial_t \int d^3r'dt' \underline{\mathbf{G}}^e(\mathbf{r}-\mathbf{r}', t-t') \cdot \mathbf{J}(\mathbf{r}', t') \\ \mathbf{H}(\mathbf{r}, t) &= \int d^3r'dt' \underline{\mathbf{G}}^h(\mathbf{r}-\mathbf{r}', t-t') \cdot \mathbf{J}(\mathbf{r}', t').\end{aligned} \tag{4}$$

In order to transform Maxwell's equations in (1) to an isotropic form we define

$$\tau = t + mz/c. \tag{5}$$

By inserting τ in (5) into Maxwell's equations in (1) we obtain

$$\begin{aligned}\nabla \times \mathbf{E}(\mathbf{r}, \tau) &= -\mu_0\mu_r\partial_\tau \underline{\boldsymbol{\alpha}} \cdot \mathbf{H}(\mathbf{r}, \tau) \\ \nabla \times \mathbf{H}(\mathbf{r}, \tau) &= \epsilon_0\epsilon_r\partial_\tau \underline{\boldsymbol{\alpha}} \cdot \mathbf{E}(\mathbf{r}, \tau) + \mathbf{J}(\mathbf{r}, \tau).\end{aligned} \tag{6}$$

Note that the rotor operator in (6) is applied only on the first ($\mathbf{r}$-) argument of $\mathbf{E}(\mathbf{r}, \tau)$ or $\mathbf{H}(\mathbf{r}, \tau)$.

We distinguish two medium speed regimes in which the medium is moving in a speed that is either under or over the medium's (at rest) phase-speed. These speed regimes are identified by either $v < c/n$ or $v > c/n$ for which α in (3) is positive or negative, respectively. In order to obtain a uniform formulation for both the under and the over phase-speed regimes, we apply here an analytic continuation of the fields for the complex $\bar{z}$ plane and define the normalized z-coordinate (cf. [12], [13])

$$\bar{z} = \sqrt{\alpha}z. \tag{7}$$

The branch cut of $\sqrt{\alpha}$ in (7) is chosen such that

$$\sqrt{\alpha} = \begin{cases}\sqrt{\alpha} & \alpha \geq 0 \\ j\sqrt{-\alpha} & \alpha < 0\end{cases} \tag{8}$$

in order to ensure the validity of the following derivation for the two speed regimes $n\beta \lessgtr 1$. The analytic continuation of the real field

$\mathbf{E}(x, y, \bar{z}, \tau)$ that is defined for real $\bar{z}$ to the upper half of the complex $\bar{z}$ plane is obtained by the convolution integral [14]

$$\breve{\mathbf{E}}(\bar{z}) = \frac{-1}{\pi j}\int_{-\infty}^{\infty} d\bar{z}' \frac{\mathbf{E}(\bar{z}')}{\bar{z}-\bar{z}'}, \quad \mathrm{Im}\,\bar{z} \geq 0 \tag{9}$$

where for simplicity we have omitted the dependence of $\mathbf{E}$ on x, y and τ. Here and henceforth, analytic fields are denoted by a breve mark ($\breve{}$). The real field is recovered from the analytic field via $\mathbf{E}(\bar{z}) = \mathrm{Re}\,\breve{\mathbf{E}}(\bar{z})$ [14].

Using these definitions we note that

$$\begin{aligned} \bar{\nabla}\times[\underline{\boldsymbol{\alpha}}^{1/2}\cdot\breve{\mathbf{H}}(\mathbf{r},\tau)] &= \sqrt{\alpha}\underline{\boldsymbol{\alpha}}^{-1/2}\cdot\nabla\times\breve{\mathbf{H}}(\mathbf{r},\tau) \\ \underline{\boldsymbol{\alpha}}^{1/2} &= \mathrm{diag}\{\sqrt{\alpha},\sqrt{\alpha},1\} \end{aligned} \tag{10}$$

where $\bar{\nabla}$ denotes the normalized del (nabla) operator

$$\bar{\nabla} = [\partial_x\hat{\mathbf{x}} + \partial_y\hat{\mathbf{y}} + \partial_{\bar{z}}\hat{\mathbf{z}}] = [\partial_x\hat{\mathbf{x}} + \partial_y\hat{\mathbf{y}} + (\sqrt{\alpha})^{-1}\partial_z\hat{\mathbf{z}}] \tag{11}$$

with $\partial_x \equiv \partial/\partial x$, and so forth. By inserting $\nabla\times\breve{\mathbf{H}}$ in (6) into (10) and applying a similar procedure to $\breve{\mathbf{E}}$, we obtain

$$\begin{aligned} \bar{\nabla}\times\breve{\bar{\mathbf{E}}}(\bar{\mathbf{r}},\tau) &= -\mu_0\mu_r\sqrt{\alpha}\partial_t\breve{\bar{\mathbf{H}}}(\bar{\mathbf{r}},\tau) \\ \bar{\nabla}\times\breve{\bar{\mathbf{H}}}(\bar{\mathbf{r}},\tau) &= \epsilon_0\epsilon_r\sqrt{\alpha}\partial_t\breve{\bar{\mathbf{E}}}(\bar{\mathbf{r}},\tau) + \breve{\bar{\mathbf{J}}}(\bar{\mathbf{r}},\tau) \end{aligned} \tag{12}$$

where we denote

$$\begin{aligned} \breve{\bar{\mathbf{E}}}(\bar{\mathbf{r}},\tau) &= \underline{\boldsymbol{\alpha}}^{1/2}\cdot\breve{\mathbf{E}}(\mathbf{r},\tau), \quad \breve{\bar{\mathbf{H}}}(\bar{\mathbf{r}},\tau) = \underline{\boldsymbol{\alpha}}^{1/2}\cdot\breve{\mathbf{H}}(\mathbf{r},\tau) \\ \breve{\bar{\mathbf{J}}}(\bar{\mathbf{r}},\tau) &= \sqrt{\alpha}\underline{\boldsymbol{\alpha}}^{-1/2}\cdot\breve{\mathbf{J}}(\mathbf{r},\tau) \end{aligned} \tag{13}$$

with $\bar{\mathbf{r}} = (x, y, \bar{z})$.

One can readily observe that the Eqs. in (12) have the form of Maxwell's equations in linear *isotropic* (free space) medium that is characterized by

$$\bar{\epsilon}_r = \sqrt{\alpha}\epsilon_r, \quad \bar{\mu}_r = \sqrt{\alpha}\mu_r, \quad \bar{c} = c/(n\sqrt{\alpha}) \tag{14}$$

where the branch cut of $\sqrt{\alpha}$ is given by (8). The dyadic GFs of (12) are obtained by using the analytic GF of the *scalar* TD wave equation [15]

$$\left[\bar{\nabla}^2 - \frac{1}{\bar{c}^2}\partial_\tau^2\right]\breve{g}(\bar{\mathbf{r}},\tau) = -\sqrt{\alpha}\delta(x)\delta(y)\breve{\delta}(\bar{z})\delta(\tau) \tag{15}$$

where $\breve{\delta}(\bar{z})$ denotes the analytic delta-function in the upper half of the complex $\bar{z}$-plane [14]

$$\breve{\delta}(\bar{z}) = \begin{cases} -(j\pi\bar{z})^{-1}, & \mathrm{Im}\,\bar{z} > 0 \\ \delta(\bar{z}) + \mathcal{P}(-j\pi\bar{z})^{-1}, & \mathrm{Im}\,\bar{z} = 0 \end{cases} \tag{16}$$

where $\mathcal{P}$ denotes Cauchy's principal value. The electric and magnetic dyadic GFs of the isotropic Maxwell's equation (12) are obtained from the analytic scalar GF via

$$\begin{aligned} \breve{\underline{\mathbf{g}}}^e(\bar{\mathbf{r}},\tau) &= \mu_r\left[\underline{\mathbf{I}} - \bar{c}^2\partial_\tau^{-2}\bar{\nabla}\bar{\nabla}\right]\breve{g}(\bar{\mathbf{r}},\tau) \\ \breve{\underline{\mathbf{g}}}^h(\bar{\mathbf{r}},\tau) &= \sqrt{\alpha}^{-1}\bar{\nabla}\times\underline{\mathbf{I}}\breve{g}(\bar{\mathbf{r}},\tau) \end{aligned} \tag{17}$$

where $\partial_\tau^{-2}g(\tau) = \int_{-\infty}^{\tau}dt'\int_{-\infty}^{t'}dt''g(t'')$.

The normalized vector fields due to the source $\breve{\bar{\mathbf{J}}}$ in (12) are given by

$$\begin{aligned} \breve{\bar{\mathbf{E}}}(\bar{\mathbf{r}},\tau) &= -\mu_0\partial_\tau\int d^3\bar{r}'\,d\tau'\breve{\underline{\mathbf{g}}}^e(\bar{\mathbf{r}}-\bar{\mathbf{r}}',\tau-\tau')\cdot\breve{\bar{\mathbf{J}}}(\bar{\mathbf{r}}',\tau') \\ \breve{\bar{\mathbf{H}}}(\bar{\mathbf{r}},\tau) &= \int d^3\bar{r}'\,d\tau'\breve{\underline{\mathbf{g}}}^h(\bar{\mathbf{r}}-\bar{\mathbf{r}}',\tau-\tau')\cdot\breve{\bar{\mathbf{J}}}(\bar{\mathbf{r}}',\tau') \end{aligned} \tag{18}$$

where $\bar{\mathbf{r}}' = (x', y', \bar{z}')$. By substituting (13) with (5) into (18) and comparing the resulting integrals with (4), we identify

$$\breve{\underline{\mathbf{G}}}^{e,h}(\mathbf{r},t) = \alpha\underline{\boldsymbol{\alpha}}^{-1/2}\cdot\breve{\underline{\mathbf{g}}}^{e,h}(\bar{\mathbf{r}},t+mz/c)\cdot\underline{\boldsymbol{\alpha}}^{-1/2} \tag{19}$$

in which $\breve{\underline{\mathbf{g}}}^{e,h}$ on the right hand side are sampled at $\bar{\mathbf{r}} = (x, y, \sqrt{\alpha}z)$. Finally, by inserting (17) into (19) and using $\mathbf{E}(\bar{z}) = \mathrm{Re}\,\breve{\mathbf{E}}(\bar{z})$, the (real) dyadic GFs are obtained directly from the analytic scalar GF $\breve{g}(\bar{\mathbf{r}},\tau)$ via

$$\underline{\mathbf{G}}^{e,h}(\mathbf{r},t) = \mathrm{Re}\left[\underline{\mathbf{L}}^{e,h}\breve{g}(\bar{\mathbf{r}},\tau)\right]\Big|_{\substack{\tau = t+mz/c \\ \bar{\mathbf{r}} = (x,y,\sqrt{\alpha}z)}} \tag{20}$$

where the differential operators $\underline{\mathbf{L}}^{e,h}$ are given by

$$\begin{aligned} \underline{\mathbf{L}}^e &= -\mu_r\bar{c}^2\partial_\tau^{-2} \\ &\quad\times\begin{bmatrix} \partial_x{}^2 - \partial_\tau^2/\bar{c}^2 & \partial_x\partial_y & \sqrt{\alpha}\partial_x\partial_{\bar{z}} \\ \partial_x\partial_y & \partial_y{}^2 - \partial_\tau^2/\bar{c}^2 & \sqrt{\alpha}\partial_y\partial_{\bar{z}} \\ \sqrt{\alpha}\partial_x\partial_{\bar{z}} & \sqrt{\alpha}\partial_y\partial_{\bar{z}} & \alpha\left(\partial_{\bar{z}}^2 - \partial_\tau^2/\bar{c}^2\right) \end{bmatrix} \\ \underline{\mathbf{L}}^h &= \begin{bmatrix} 0 & -\partial_{\bar{z}}/\sqrt{\alpha} & \partial_y \\ \partial_{\bar{z}}/\sqrt{\alpha} & 0 & -\partial_x \\ -\partial_y & \partial_x & 0 \end{bmatrix}. \end{aligned} \tag{21}$$

In view of (20), (15) is solved subject to the causality condition

$$\breve{g}(\bar{\mathbf{r}}, t+mz/c) = 0, \quad t < 0. \tag{22}$$

B. Speed Regimes

Next we follow the procedure in (20)–(22) and obtain the 3D dyadic GFs in the under and over phase-speed regimes.

1) Under Phase-Speed Regime: In this speed regime $\bar{z}$ is real. Thus $\underline{\mathbf{G}}^{e,h}(\mathbf{r},t)$ in (20) are obtained by applying the (real) operators $\underline{\mathbf{L}}^{e,h}$ to the real scalar GF $g(\bar{\mathbf{r}},\tau) = \mathrm{Re}\,\breve{g}(\bar{\mathbf{r}},\tau)$ which is identified from the real part of (15) as the 3D scalar free-space TD GF

$$g(\bar{\mathbf{r}},\tau) = \sqrt{\alpha}\frac{\delta(\tau-\bar{R}/\bar{c})}{4\pi\bar{R}}, \quad \bar{R} = \sqrt{x^2+y^2+\bar{z}^2}. \tag{23}$$

By setting $\tau = t + mz/c$ in $g(\bar{\mathbf{r}},\tau)$ in (23), we note that the scalar GF satisfies the causality condition in (22). The resulting dyadic GFs in this speed regime are identical to those which were obtained in [1]. The wavefront is obtained by setting the Dirac delta function argument in (23) to zero. By inserting $\tau = t + mz/c$, we obtain the ellipsoid

$$\begin{aligned} &\left(\frac{\rho}{B}\right)^2 + \left(\frac{z-z_c}{A}\right)^2 = 1, \quad z_c = \frac{n^2-1}{n^2-\beta^2}\beta ct \\ &A = \frac{1-\beta^2}{n^2-\beta^2}nct, \quad B = \sqrt{\frac{1-\beta^2}{n^2-\beta^2}}ct \end{aligned} \tag{24}$$

where $\rho^2 = x^2 + y^2$.

2) Over Phase-Speed Regime: In the over phase-speed regime, $\alpha < 0$ and therefore $\bar{z}$ and $\bar{c}$ are imaginary numbers. In this regime we define *real* longitudinal coordinate and phase-speed by

$$\bar{z}_i = \sqrt{-\alpha}z, \quad \bar{c}_i = c/(n\sqrt{-\alpha}), \quad \alpha < 0. \tag{25}$$

By using $\bar{z} = j\bar{z}_i$ and $\sqrt{\alpha} = j\sqrt{-\alpha}$ we obtain the differential operators in (21)

$$\begin{aligned}\underline{\mathbf{L}}^e &= \mu_r \bar{c}_i^2 \partial_\tau^{-2} \\ &\quad \times \begin{bmatrix} \partial_x{}^2 + \partial_\tau^2/\bar{c}_i^2 & \partial_x\partial_y & \sqrt{-\alpha}\partial_x\partial_{\bar{z}_i} \\ \partial_x\partial_y & \partial_y{}^2 + \partial_\tau^2/\bar{c}_i^2 & \sqrt{-\alpha}\partial_y\partial_{\bar{z}_i} \\ \sqrt{-\alpha}\partial_x\partial_{\bar{z}_i} & \sqrt{-\alpha}\partial_y\partial_{\bar{z}_i} & -\alpha\left(\partial_{\bar{z}_i}^2 - \partial_\tau^2/\bar{c}_i^2\right) \end{bmatrix} \\ \underline{\mathbf{L}}^h &= \begin{bmatrix} 0 & \partial_{\bar{z}_i}/\sqrt{-\alpha} & \partial_y \\ -\partial_{\bar{z}_i}/\sqrt{-\alpha} & 0 & -\partial_x \\ -\partial_y & \partial_x & 0 \end{bmatrix}. \end{aligned} \tag{26}$$

The 3D dyadic GFs in (20) are obtained by operating with the (real) operators $\underline{\mathbf{L}}^{e,h}$ over the scalar $\breve{g}(\bar{\mathbf{r}}_i, \tau)$ in (15). Therefore we can substitute the analytic GF with its real part $g(\bar{\mathbf{r}}_i, \tau) = \mathrm{Re}\,\breve{g}(\bar{\mathbf{r}}_i, \tau)$. By taking the real part of (15) and using (16) we obtain the differential equation

$$\left[\partial_x^2 + \partial_y^2 - \partial_{\bar{z}_i}^2 + \frac{1}{\bar{c}_i^2}\partial_\tau^2\right] g(\bar{\mathbf{r}}_i, \tau) = -\sqrt{-\alpha}\delta(\bar{\mathbf{r}}_i)\delta(\tau) \tag{27}$$

where $\bar{\mathbf{r}}_i = (x, y, \bar{z}_i)$. Here the medium speed exceeds the phase-speed in the comoving frame so the causality condition in (22) can be manifested by

$$g(\bar{\mathbf{r}}_i, \tau)|_{\bar{z}_i < 0} = 0. \tag{28}$$

The solution for $g(\bar{\mathbf{r}}_i, \tau)$ in (27) subject to (28) can be obtained by applying the temporal Fourier transform to (27) and solving the resulting 2D Klein-Gordon equation as in [16] (see also [13]). By applying the inverse Fourier transform we obtain

$$g(\bar{\mathbf{r}}_i, \tau) = \sqrt{-\alpha}\left[\frac{\delta(\tau + \bar{R}_i/\bar{c}_i) + \delta(\tau - \bar{R}_i/\bar{c}_i)}{4\pi\bar{R}_i}\right] H(\bar{z}_i - \rho) \tag{29}$$

where $\bar{R}_i = \sqrt{\bar{z}_i^2 - \rho^2}$ and $H()$ denotes the Heaviside (unit step) function. The wavefront of the scalar GF in (29) is given by

$$t + mz/c = \pm\bar{R}_i/\bar{c}_i. \tag{30}$$

By inserting m in (2) into (30), we obtain the ellipsoid in (24). Note that the scalar Green's function in (29) consists of two wavefronts in $(\mathbf{r}_i, \tau)$ space which propagate towards and away from the source at $\bar{\mathbf{r}}_i = 0$. Nevertheless, the time shift of $\tau = t + mz/c$ in (20) yields *causal* dyadic GFs that propagate in $(\mathbf{r}, t)$ space away from the source and satisfy the causality condition in (22).

Note that the scalar GF in (29) is different than the one that was obtained in [2], [3] in which only the second delta function is present. Tai has used the condition in (30) without the $\pm$ signs in order to obtain the wavefront. By squaring both sides of his condition he added the half ellipsoid which was not present in his GF solution and by that Tai has arrived at the wavefront in (24) [see also Fig. 2].

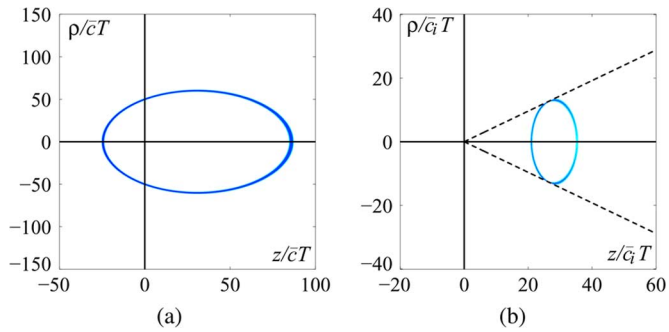

Fig. 1. The scalar Green's function $g(\bar{\mathbf{r}}, t + mz/c)$ for $n = 1.5$ sampled at $t = 50T$. (a) Under phase-speed regime in (23) for $\beta = 0.5$. (b) Over phase-speed regime in (29) for $\beta = 0.9$.

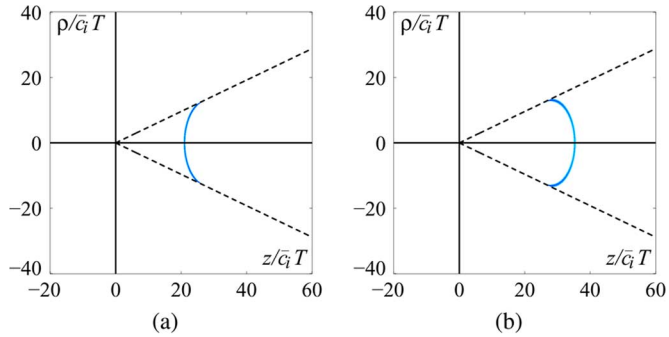

Fig. 2. Contributions of (a) the first and (b) the second terms of the scalar GF in Fig. 1(b). The wavefront which is plotted in Fig. 2(a) is not present in the scalar GF that was derived in [2], [3].

In order to demonstrate the wave phenomena associated with the GFs we replace the impulsive time-dependence in (23) and (29) by a Lorentzian pulse of

$$f(\tau) = \frac{1}{\pi}\frac{T/2}{\tau^2 + (T/2)^2} \tag{31}$$

which models a short-pulse with T being its temporal pulse width. The scalar GF $g(\bar{\mathbf{r}}, t + mz/c)$ in (20) is plotted in Fig. 1 for $n = 1.5$ and $t = 50T$ for the two speed regimes; Fig. 1(a) in the under phase-speed regime for $\beta = 0.5$, and Fig. 1(b) in the over phase-speed regime for $\beta = 0.9$. The spatial coordinates (ρ, z) are normalized with respect to $\bar{c}T$ in Fig. 1(a) and with respect to $\bar{c}_i T$ in Fig. 1(b).

The under phase-speed GF in Fig. 1(a) demonstrates propagation in all directions away from the source location in $\mathbf{r} = 0$. The medium velocity in the z direction causes an asymmetric propagation over the ellipsoid in (24). In the over phase-speed regime the scalar Green's function in (29) resides within the conical region $\bar{z}_i > \rho$. By using (25), we identify this region to be $\tan\theta < \sqrt{-\alpha}$ where θ is the conventional spherical angle of $\mathbf{r}$ with the z-axis and α is given in (3). This condition is a manifestation of the Čerenkov radiation. The contour $\bar{z}_i = \rho$ is plotted in Fig. 1(b) by a dashed line.

Finally in Fig. 2(a) and (b), we plot the contributions of the first and the second terms in (29), respectively, which are samples at $\tau = t + mz/c$. These terms are identified as the left and right directed propagation of the source, which due to the medium z directed velocity that exceeds the phase-speed, are propagating in the positive z direction

with different velocities. The wavefront in Fig. 2(a) is not present in the solution that was derived in [2], [3].

REFERENCES

[1] R. T. Compton, "The time dependent Green's function for electromagnetic waves in moving simple media," *J. Math. Phys.*, vol. 7, pp. 2145–2152, 1966.

[2] C. T. Tai, "Time dependent Green's function for a moving isotropic nondispersive medium," *J. Math. Phys.*, vol. 8, pp. 646–647, 1967.

[3] C. T. Tai, "Transient radiation in a moving isotropic medium," *J. Electromagn. Waves Appl.*, vol. 7, pp. 1–11, 1993.

[4] C. T. Tai, "The dyadic Greens function for a moving isotropic medium," *IEEE Trans. Antennas Propag.*, vol. 13, pp. 322–323, 1964.

[5] K. S. H. Lee and C. H. Papas, "Electromagnetic radiation in the presence of moving simple media," *J. Math. Phys.*, vol. 5, pp. 1668–1672, 1964.

[6] R. T. Compton and C. T. Tai, "Radiation from harmonic sources in a uniformly moving medium," *IEEE Trans. Antennas Propag.*, vol. 13, pp. 574–577, 1965.

[7] J. Van Bladel, *Relativity and Engineering*. New York: Springer, 1984.

[8] A. Lakhtakia and W. S. Weiglhofer, "On electromagnetic fields in a linear medium with gyrotropic-like magnetoelectric properties," *Microw. Opt. Techn. Let.*, vol. 15, pp. 168–170, 1997.

[9] T. G. Mackay and A. Lakhtakia, "Negative phase velocity in a uniformly moving, homogeneous, isotropic, dielectric-magnetic medium," *J. Phys. A, Math. Gen.*, vol. 37, pp. 5697–5711, 2004.

[10] A. Lakhtakia and T. G. Mackay, "Simple derivation of dyadic Green functions of a simply moving, isotropic, dielectric-magnetic medium," *Microw. Opt. Techn. Let.*, vol. 48, pp. 1073–1074, 2006.

[11] T. G. Mackay, A. Lakhtakia, and S. Setiawan, "Positive-, negative-, and orthogonal-phase-velocity propagation of electromagnetic plane waves in a simply moving medium," *Optik*, vol. 118, pp. 195–202, 2007.

[12] A. Lakhtakia and T. G. Mackay, "Dyadic Green function for an electromagnetic medium inspired by general relativity," *Chinese Phys. Lett.*, vol. 23, pp. 832–833, 2006.

[13] T. Danov and T. Melamed, "Spectral analysis of relativistic dyadic Green's function of a moving dielectric-magnetic medium," *IEEE Trans. Antennas Propag.*, vol. 59, pp. 2973–2979, 2011.

[14] E. Heyman and T. Melamed, "Space-time representation of ultra wideband signals," in *Advances in Imaging and Electron Physics*. The Netherlands: Elsevier, 1998, vol. 103, pp. 1–63.

[15] L. B. Felsen and N. Marcuvitz, *Radiation and Scattering of Waves*. Piscataway, NJ: IEEE Press, 1994, Classic reissue.

[16] M. H. Cohen, "Radiation in a plasma. I. Čerenkov effect," *Phys. Rev.*, vol. 123, pp. 711–721, Aug. 1961.

Fast 3D-ISAR Image Simulation of Targets at Arbitrary Aspect Angles Through Nonuniform Fast Fourier Transform (NUFFT)

Xin Yi He, Xiao Yang Zhou, and Tie Jun Cui

***Abstract*—We present a method to generate three-dimensional (3D) inverse synthetic aperture radar (ISAR) images of a target at arbitrary aspect angles using the shooting and bouncing ray (SBR) method. We have derived a 3D-image-domain ray-tube integration formula based on the SBR technique. The imaging formula is in a form of convolution, then a nonuniform fast Fourier transform (NUFFT) is induced to achieve the convolution, which can be used to generate 3D ISAR images rapidly. Compared to the conventional algorithm where the ISAR images are obtained by inverse Fourier transforming the computed scattered fields over a range of frequencies and a range of aspect angles, the new formula needs only one-time ray tracing and physical optics (PO) integration over a small angle span. Hence the computational time is decreased tremendously. The ISAR images of a missile target and an armored car for several aspect angles are presented to demonstrate the efficiency and accuracy of the proposed method.**

***Index Terms*—Electromagnetic modeling and simulation, electromagnetic scattering, inverse synthetic aperture radar image, shooting and bouncing rays, 3D nonuniform fast Fourier transform.**

I. INTRODUCTION

Synthetic aperture radar (SAR) and inverse synthetic aperture radar (ISAR) are instantaneous sensors, which have been widely used in the complicated civilian and battle environments for the ability to work under almost all weather conditions. The technology of ISAR-image simulations of targets and environment can be combined with the computer graphics and modern computational electromagnetics, which has provided a powerful tool for the process, explanation and applications of SAR and ISAR images.

Simulation of ISAR-image based on electromagnetic (EM) model, either the full-wave numerical technique [1] or high-frequency simulation method [2], always should computer the far scattered fields over a band of angles and frequencies. Such simulation data are fan-shaped arranged in the 2D spatial-frequency domain, then are interpolated into a rectangular domain. This process is called as the polar format algorithm (PFA). The fast Fourier transform (FFT) is then used to reconstruct the image [3]. The whole scheme is called as the PFA-FFT method in the remaining part of the communication. It is rather time consuming to obtain high-resolution images of a complicated target. A significant contribution was made by Ling *et al.*, who derived the image-domain ray tube integration formula for the shooting and bouncing ray (SBR) technique [4]–[6]. The image formation is under the concept of the equivalence between the bistatic and monostatic radar cross sections (RCSs) in a small angle approximation. The formation gives the contribution of each ray to the overall ISAR image directly. The formation is furthermore reorganized as a convolution form and can be performed by

Manuscript received April 05, 2011; revised October 03, 2011; accepted October 10, 2011. Date of publication March 01, 2012; date of current version May 01, 2012. This work was supported in part by the 973 Project under Grant No. 613151, and in part by the National Science Foundation of China under Grant Nos. 60802001 and 60972121.

The authors are with the Institute of Target Characteristics and Identification and the State Key Laboratory of Millimeter Waves, School of Information Science and Engineering, Southeast University, Nanjing 210096, China (e-mail: tjcui@seu.edu.cn).

Color versions of one or more of the figures in this communication are available online at http://ieeexplore.ieee.org.

Digital Object Identifier 10.1109/TAP.2012.2189717